The Application of Femtosecond Time-Resolved Coherent Anti-Stokes Raman Scattering for the Investigation of Ground and Excited State Molecular Dynamics of Molecules in the Gas Phas...

4 AUTHORS, INCLUDING:

Gregor Knopp
Paul Scherrer Institut
80 PUBLICATIONS   747 CITATIONS

SEE PROFILE

Arnulf Materny
Jacobs University
198 PUBLICATIONS   2,336 CITATIONS

SEE PROFILE

Wolfgang Kiefer
University of Wuerzburg
881 PUBLICATIONS   9,877 CITATIONS

SEE PROFILE

The Application of Femtosecond Time-Resolved Coherent Anti-Stokes Raman Scattering for the Investigation of Ground and Excited State Molecular Dynamics of Molecules in the Gas Phase

M. Schmitt, G. Knopp, A. Materny, and W. Kiefer*

Institut für Physikalische Chemie der Universität Würzburg, Am Hubland, D-97074 Würzburg, Federal Republic of Germany

In this study, we have employed femtosecond time-resolved CARS (coherent anti-Stokes Raman scattering) spectroscopy in order to gain information about the molecular dynamics evolving on the electronic excited as well as ground state potential energy surfaces (PES) of iodine and bromine in the gas phase. The coherences of the wave packet in the temporal transients of the molecules excited by the ultrashort laser pulses are analyzed by means of fast Fourier transform calculations as well as by a simple model describing the purely rotational contribution. The latter is able to describe the rotational coherence seen for the excited but not for the ground-state dynamics. Information about vibrational dynamics is extracted from the transients reflecting the wave packet motion on both the ground and excited-state PES.

1. Introduction

Ultrafast molecular vibrations and rotations are the fundamental motions that characterize chemical bonding and determine the reaction dynamics at the molecular level. The time scales for these motions are typically 100 fs for vibrations and 100 ps for rotations. Recent advances in time-domain spectroscopy have enabled spectroscopists to capture chemical processes directly on the time scale of the fastest elementary steps.[1−3] Ultrashort laser pulses with a duration of less than about 100 fs allow for a coherent broadband excitation with preparation and detection of vibrational superposition states. The time evolution of these rovibrational wave packets in the ground as well as electronically excited state give information on the molecular dynamics. There are different possibilities for studying the molecular dynamics in real time. Typically, the linear response to the optical field in a two-pulse pump−probe scheme is used in order to initiate and probe the wave packet in a certain quantum state.[2−4] In such experiments, the signal detection was performed by laser-induced fluorescence (LIF),[5−7] absorption,[8−10] resonant impulsive stimulated Raman scattering (RISRS),[11] stimulated emission pumping,[12] multiphoton ionization (MPI),[13,14] photoelectron kinetic energy,[15] and zero kinetic energy (ZEKE),[16] and by several other methods such as, for example, femtosecond up conversion.[17]

Since Leonhardt et al.[18] applied femtosecond laser pulses to the observation of time-resolved coherent anti-Stokes Raman scattering (CARS), several groups have reported sub-picosecond and femtosecond time-resolved CARS measurements.[19−25] Theories for these time-resolved nonlinear spectroscopical methods were developed by several researchers.[21,26−29] Time-resolved coherent Raman scattering techniques have been widely employed in condensed-phase studies of vibrational dephasing.[18,30−40] However, these methods have not been exploited on the sub-picosecond time scale for gas-phase studies until recently Hayden and Chandler[25] reported the application of femtosecond time-resolved coherent Raman techniques to excite and monitor the evolution of vibrational coherence in gas-phase samples of benzene as well as 1,3,5-hexatriene. Recently, nonlinear four-wave mixing (FWM) techniques were incorporated in different temporal pulse schemes to extract the dynamics of atomic, unimolecular, and bimolecular systems in the gas phase by Zewail and co-workers.[41] For the FWM a three-dimensional forward geometry (folded BOXCARS arrangement)[42−44] was chosen. Degenerate FWM (DFWM) as well as a two-color grating experiment[45] were used to replace the probe pulse in a pump−probe scheme. Also the FWM process itself was used to gain information on the decay dynamics of atomic Na.

Very recently, first results were published introducing femtosecond time-resolved CARS spectroscopy applied to the investigation of molecular dynamics in gases.[46] There, it was demonstrated that by this method one can observe the dynamics of a wave packet either evolving on the ground or on the excited-state potential energy surface (PES). Depending on the timing of the three laser pulses giving rise to the CARS signal, the resulting transients show the characteristics of the rovibrational behavior of the molecule in the ground and excited state. As will be shown in the following, the wave packet prepared on the excited-state PES by a pump laser pulse can be probed by the coherent interaction with the contemporaneous second pump and Stokes laser pulse for different time delays. On the other hand, a pump laser pulse together with the Stokes laser pulse are capable of preparing a wave packet on the electronic ground-state PES, which afterward can be probed by the second pump laser interaction. In both cases the coherent CARS signal could be detected using a folded BOXCARS arrangement giving rise to background-free transients as well as high selectivity. In this contribution we will give some more details concerning the time-resolved CARS technique applied. We will discuss results obtained from experiments on both iodine and bromine vapor. A theoretical interpretation by means of a nonperturbative evaluation scheme for the nonlinear polarization[47] will be given in a forthcoming paper.[48]

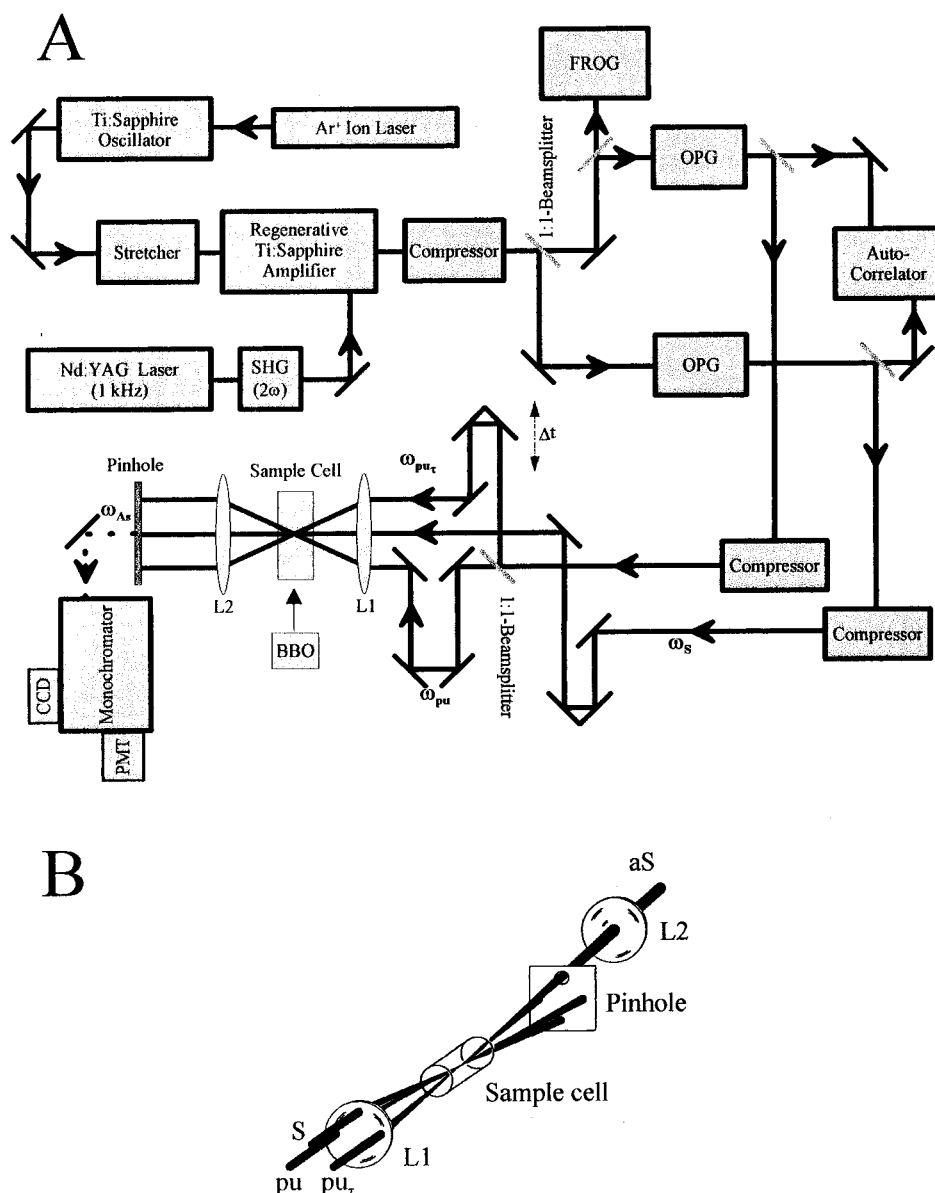* To whom correspondence should be addressed.

Figure 1. Experimental setup showing (A) the femtosecond laser system and (B) the beam path of the BOXCARS arrangement. Computer controlled actuators were used to vary the relative arrival time of the femtosecond pulses. Only one actuator (Δt) was moved in the experiment to obtain a transient.

2. Experimental Section

The setup used for the femtosecond CARS experiments is shown in Figure 1A and is described in the following. The laser system is based on a Ti:Sapphire oscillator (Coherent MIRA) pumped by the multiline output of an Ar^+ ion laser (Coherent Innova 310) running at about 8 W. The pulses were produced by the oscillator at a repetition rate of 83 MHz having temporal pulse widths of about 100 fs. The pulse energy was less than 10 nJ and the pulses were centered at about 800 nm having a spectral width (fwhm) of 14 nm. For the amplification of the pulses a regenerative Ti:Sapphire amplifier system (Clark-MXR) was used. The pulses were stretched to a duration of >200 ps before amplification. The regenerative Ti:Sapphire amplifier was pumped by a frequency doubled Nd:YAG laser at a repetition rate of 1 kHz. After recompression, the pulses had energies of about 1.0 mJ and temporal widths of less than 100 fs.

To have two different colors available, the 800 nm pulse train was split into two parts by means of a beam splitter. Using two four-path OPAs (optical parametric amplifiers, Light Conversion) two independent wavelengths could be chosen. The laser pulses were produced using sum frequency generation between signal and idler output of the OPA as well as second harmonic generation of either the signal or the idler light. The pulses were finally compressed in double-pass two-prism arrangements resulting in temporal pulse widths of about 70 fs (assuming Gaussian pulse profiles).

One of the OPA outputs was branched by a 1:1 beam splitter to produce the two pump pulses pu and pu_τ. The two pump beams were then aligned parallel to one another and spatially overlapped at the common focus in the sample cell by the achromatic lens L1. The Stokes beam S (output of the second OPA) was aligned parallel to and spatially separated from the two pump pulses and passed through the top of lens L1, focusing in the same region as the two pump beams. This folded BOXCARS configuration (see also part B of Figure 1) was employed in order to separate the signal from the incoming
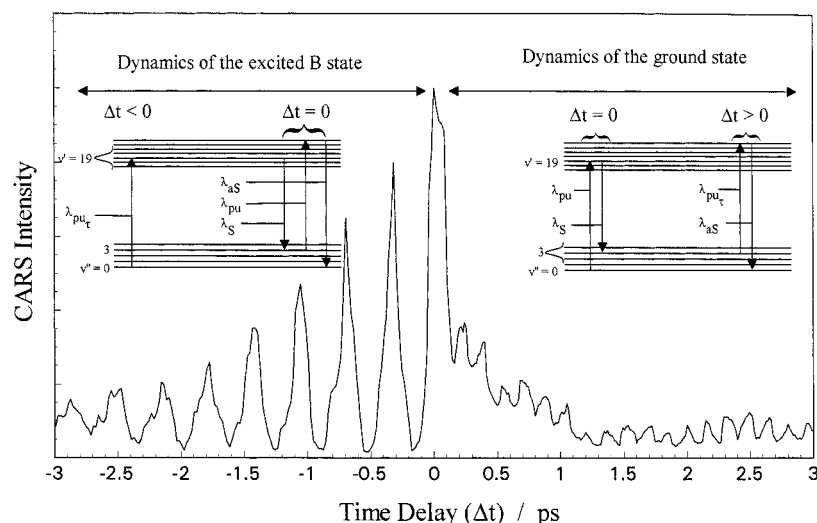
Molecular Dynamics of Molecules in the Gas Phase

J. Phys. Chem. A, Vol. 102, No. 23, 1998 **4061**

Figure 2. Femtosecond CARS transient obtained for pump wavelengths $\lambda_{pu} = \lambda_{pu_\tau} = 559$ nm and a Stokes wavelength $\lambda_S = 579$ nm detecting the CARS signal at $\lambda_{aS} = 539$ nm. The wave packet dynamics in the B sate (negative delay times, $\Delta t < 0$) as well as in the ground state (positive delay times, $\Delta t > 0$) of iodine can be resolved. Energy diagrams of the CARS process are shown as inserts for both cases $\Delta t < 0$ and $\Delta t > 0$, indicating the relative timing of the laser pulses.

pump and probe beams.[44] In this geometry the phase-matching condition is fulfilled.

The pump pulses and the probe pulses could be delayed in time relative to each other by means of Michelson interferometer arrangements. In the experiments presented in this paper, the pump pulse pu and the Stokes pulse S were kept temporally overlapped and fixed. The CARS transients were recorded as a function of delay time Δt between the pump pulse pu_τ and the two fixed and time coincident pulses pu and S. The relative timing between the different pulses was varied with a computer-controlled actuator that allowed for optical delay up to 3 ns with a minimal stepsize of 6 fs. The determination of the position of temporal overlap (time zero) between the different beam pairs was made using a cross correlation setup with second harmonic generation as well as sum frequency mixing in a thin, phase-matched BBO crystal.

The femtosecond CARS signal pulse aS (aS = anti-Stokes) generated in the sample cell travels in a direction determined by the phase-matching condition. This direction is different from that of the incident laser beams (see Figure 1B), and the signal could thus be easily separated by a spatial filter. The CARS signal beam was collimated by a second achromatic lens L2. After the straylight was separated from the CARS signal by means of a monochromator (Acton SpectraPro-500), the anti-Stokes signal was detected by a fast photomultiplier tube (RCA C31024 A). The signal-to-noise ratio was enhanced by use of a boxcar−integrator (EG&G model 4121B) in-gated−integrator mode, as well as by numerical averaging of several pulses.

3. Results and Discussion

In this section we discuss results obtained from experiments performed on iodine and bromine vapor. We start with results for I_2 which was already studied by several other groups (see, e.g., ref 2 and references therein) using different methods.

Figure 2 shows the experimental CARS intensity as a function of delay time Δt between the pump pulse (pu_τ) and the two time coincident pulses pu and S for I_2 vapor. The signal exhibits well defined beats for negative delay times with a separation of about 380 fs, corresponding to a vibrational energy spacing of 88 cm^{-1}. This agrees well with the experimental vapor phase vibrational energy spacing in the excited B state at the energy accessed by the 559 nm pump laser. For positive delay times

the signal shows oscillations at about twice the frequency of the oscillations at negative delay times. The oscillations at $\Delta t > 0$ arise from ground-state vibrational beats.

This can be explained by considering the energy level diagrams responsible for these two processes, which are shown in Figure 2. Three laser fields interact with the ensemble of I_2 molecules. Two laser pulses have the same wavelength, $\lambda_{pu} = \lambda_{pu_\tau}$. The third laser pulse (S) is tuned to a lower wavelength λ_S in such a way that the difference between pump and Stokes laser wavelength is resonant with a vibrational Raman transition in the molecule. For iodine the wavelength difference was tuned to the second overtone $\Delta v'' = 3$. While one of the pump pulses (pu) and the Stokes pulse S are coincident in time ($\Delta t = 0$), the second pump pulse pu_τ arrives having a variable time delay.

In the case that pu_τ comes before the time coincident pulses pu and S, the CARS signal reveals the evolution of the vibrational and rotational coherence of the excited B-state wave functions. Here, the first pulse (pu_τ) creates a wave packet in the excited B-state. After a variable time delay ($\Delta t < 0$) this wave packet is probed by the coherent interaction with the pu and S pulses giving rise to the coherent anti-Stokes Raman scattering signal.

If, on the other hand, the pump pulse (pu_τ) arrives later ($\Delta t > 0$) than the other two pulses (pu and S), the CARS signal reflects the dynamics in the electronic ground state. In this case the two time coincident laser pulses (pu and S) prepare a wave packet in the electronic ground state which is probed by the time delayed third laser pulse (pu_τ), observing the coherent anti-Stokes Raman scattering.

In Figure 3A and Figure 4A we show CARS transients obtained for I_2 taken over longer delay times. Figure 3A gives the long time behavior for negative ($\Delta t < 0$) and Figure 4A that for positive ($\Delta t > 0$) delay times. The peak for $\Delta t = 0$ is not considerably higher than what one would expect from the decay behavior of the oscillations of the excited state. This means that the so-called coherent artifact, which was discussed, for example, in ref 49, plays a minor role in our experiment and that resonant contributions are dominating the CARS transients of iodine. To analyze the experimental data shown in part A of Figures 3 and 4, we give the results of a fast Fourier transform (FFT) of the transients in the corresponding parts B. In both FFT spectra peaks at low wavenumbers (about 5 cm^{-1}
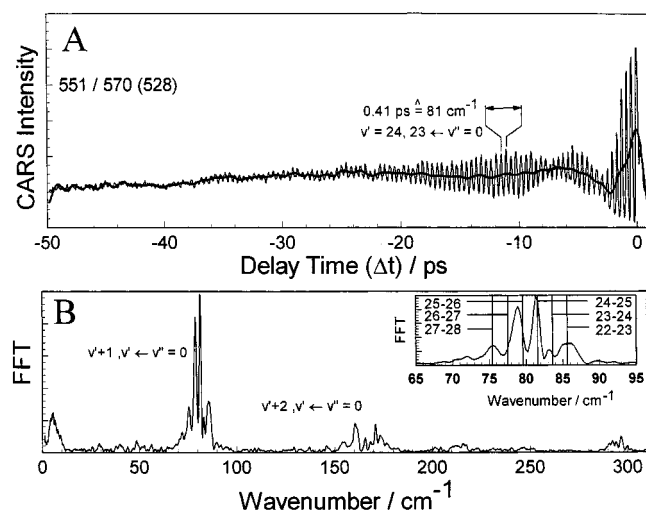
Figure 3. (A) Femtosecond time-resolved CARS transient showing the wave packet dynamics in the excited B state of iodine ($\lambda_{pu} = \lambda_{pu_r}$ = 551 nm, λ_S = 570 nm, λ_{aS} = 528 nm) and (B) the result of a fast Fourier transform of this transient. The insert shows the band due to transitions $v' \leftarrow v'' = 0$ and $v'+1 \leftarrow v'' = 0$ in detail. The thick line shown in part A is the low-frequency contribution to this transient obtained from fast Fourier transform calculations.
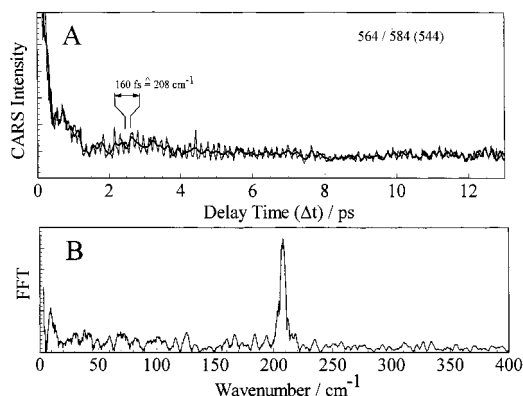

Figure 4. (A) Femtosecond time-resolved CARS transient showing the wave packet dynamics in the ground state of iodine ($\lambda_{pu} = \lambda_{pu_r}$ = 564 nm, λ_S = 584 nm, λ_{aS} = 544 nm) and (B) the result of a fast Fourier transform of this transient. The thick line shown in part A is the low-frequency contribution to this transient obtained from fast Fourier transform calculations.

for the excited and 10 cm^{-1} for the ground state transient in Figures 3B and 4B, respectively), appear. We assign these features to the rotational dynamics of the molecules. To demonstrate the effect of these low frequency contributions on the transient shape, we removed all components at higher wavenumbers from the FFT spectra and performed a transform back to the time domain. The results are shown in Figures 3A and 4A (thick lines) for the excited and ground state transients, respectively. Figure 5 shows the transients after subtraction of the low-frequency contributions (part A, excited state; part B, ground state). It is obvious that the slow modulation of the transients at early times (as to be expected) are determined by the low-frequency part of the FFT spectra. We do not have an explanation for the fine structure seen for the low-frequency contribution shown in Figure 4A. Theoretical calculations are in progress and will make a further interpretation possible.[48]

The general shape of the transients is determined by the quantum coherence of vibrations and rotations of the molecules excited. The influence of these coherences on the shape of the time dependent signal has been discussed in a number of articles.[50-56] Assuming that the excitation starts from a single
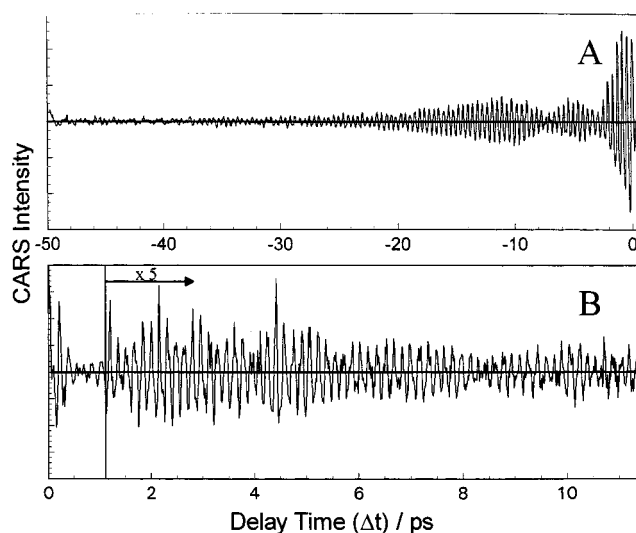

Figure 5. (A) Result of a subtraction of the low-frequency contribution from the excited-state transient, both shown in Figure 3A. (B) Same for the ground-state transient shown in Figure 4A. The resulting transients show the vibrational coherences of the two different electronic states.

rovibrational level of the electronic ground-state characterized by the quantum numbers (v'' and J''), in a simple picture one has to consider the following final states in the electronic excited state: (v_i and J_i') and (v_j and J_j') where due to the $\Delta J = \pm 1$ selection rules $J' = J'' \pm 1$. Furthermore, we assume $v_j' \neq v_i'$. After some calculation, one finds two contributions to the transient intensity:[56] (i) an oscillatory part

$$I_V(t) \propto \sum_{i,j} A_{Vij} \cos(2\pi c[E(v_i') - E(v_j')]\Delta t) \qquad (1)$$

and (ii) a rotational part

$$I_R(t) \propto \frac{J(J+1)}{2J+1} \cos(2\pi c[E(J''+1) - E(J''-1)]\Delta t) \qquad (2)$$

To include more states, a summation over all accessed J and v has to be performed weighted by a Boltzmann factor as well as by the spectral shape of the laser pulse. If for the polarization of the pump and probe pulses magic-angle conditions[57] are fulfilled, no contribution due to rotational anisotropy (eq 2) can be detected. However, the lasers in our experiment were all polarized parallel to each other resulting in transient shapes determined by both vibrational and rotational coherences.

Using the simple model for the rotational coherence, we are able to simulate the decay behavior seen for short delay times as well as the rotational recurrences for the excited-state dynamics. The rotational recurrences appear after delay times (>500 ps) which are not accessed in our experiments. Figure 6 shows a comparison between the calculated low-frequency contributions of the experimental transient (upper curve) given in Figure 3A and the simulated short time behavior (lower curve) for the excited state dynamics. Having in mind the rather crude approximations made for the calculations, we fit the theoretical curve to the shape of the FFT result fairly well. However, we were not able to simulate the contributions of rotational coherence seen for the ground state. A reason for this might be that the model applied does not consider the influence of the Franck Condon factors which certainly plays an important role for the calculation of the "pump−dump" process responsible for the preparation of the ground state wave packet.

Molecular Dynamics of Molecules in the Gas Phase

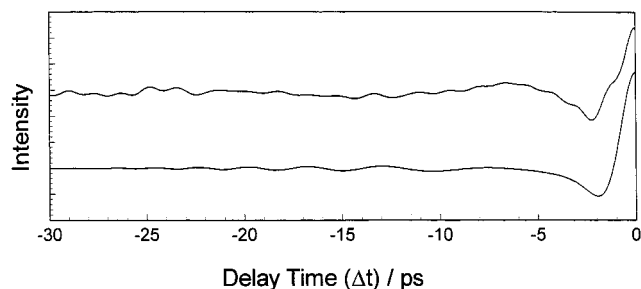*J. Phys. Chem. A, Vol. 102, No. 23, 1998* **4063**

Figure 6. The upper curve shows the low frequency contribution to the excited state transient taken from iodine which is also shown in Figure 3A. It was obtained from fast Fourier transform calculations (compare Figure 5A). The lower curve is the purely rotational coherence as calculated from the simple model described in the text.
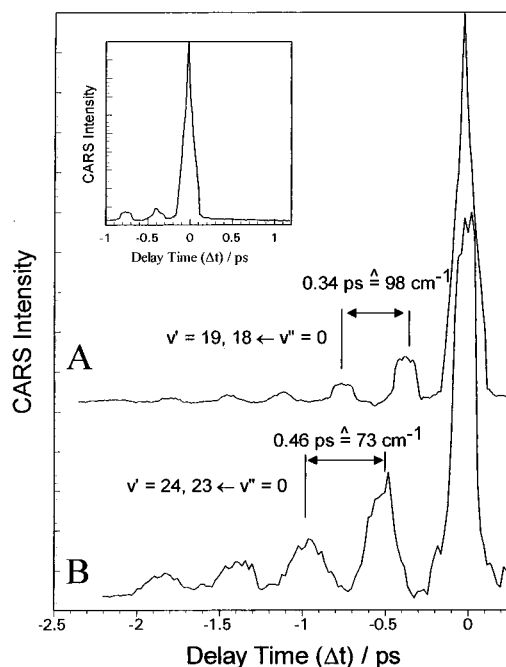

Figure 7. Femtosecond time-resolved CARS transients showing the wave packet dynamics in the excited B state of bromine. (A) CARS transient for $\lambda_{pu} = \lambda_{pu_r} = 548$ nm, $\lambda_S = 557$ nm, $\lambda_{aS} = 538$ nm; (B) $\lambda_{pu} = \lambda_{pu_r} = 535$ nm, $\lambda_S = 544$ nm, $\lambda_{aS} = 525$ nm. The insert shows the transient (A) also for positive delay times.

Besides the purely rotational coherence effects, the CARS transients also show the average vibrational frequencies as well as beat patterns due to both the local anharmonicity constants and the rotation−vibration coupling. The excited-state signal (Figure 3A) shows oscillations with a period of about 410 fs, corresponding to a vibrational wavenumber spacing of about 81 cm^{-1}. This value agrees with the experimental vibrational energy spacings (vapor phase) in the B state around $v' = 24$,[58,59] which is reached by the $\lambda_{pu} = 551$ nm laser pulse from the ground state. The Fourier spectrum of the CARS transient in Figure 3A shown in Figure 3B is consistent with this analysis. Closer inspection of the transform reveals several peaks, corresponding to different vibrational levels excited. Due to a coherent excitation of vibrational energy levels with $\Delta v' = 1$ and 2, we find in the Fourier spectrum components at about 80 and 160 cm^{-1}, respectively. The insert of Figure 3B shows the wavenumber differences of transitions $v' \leftarrow v'' = 0$ and $v' + 1 \leftarrow v'' = 0$ in detail. The resolved components agree well with the wavenumber positions of the lines observed in frequency domain experiments.[58,59]

For the CARS experiment we have chosen a wavenumber difference between pump and Stokes laser corresponding to the second overtone of the I_2 ground-state vibration. The FFT spectrum of the ground-state CARS transient shown in Figure 4B reveals a band at about 208 cm^{-1}. Comparing this wavenumber position to wavenumber differences calculated on the basis of RKR values of the electronic ground state taken from ref 60 shows that the electronic ground state is prepared around $v'' = 3$. That is exactly what could be expected from the experimental conditions as mentioned above.

The modulation of the envelopes of the vibrational transients (compare Figure 5) is mainly determined by the anharmonicity of the potential energy surfaces (PES). This results in a plainly different appearance of the ground and excited-state transients. The excited B state of iodine is very anharmonic in the range of the vibrational levels accessed. Therefore, the measured oscillations of the wave packet prepared in the excited B state show clear dephasing and rephasing patterns (Figure 5A). However, the ground-state wave packet is prepared around $v' = 3$ where the shape of PES is close to harmonic. Therefore, the amplitudes of the oscillations seen probing the ground-state dynamics do show much less modulation due to dephasing and rephasing on the considered time scale (Figure 5B).

Additionally, the damping of the amplitudes due to rotation−vibration interaction results in vanishing signal intensities after about 40 ps for the excited state (Figure 5A). On the other hand, the amplitudes of the vibrational modulation seen for the ground-state transient do decrease slower (Figure 5B). While the coupling constants α_e are about the same for the excited B

state[61] and the ground state,[59] considerably higher vibrational levels are involved in the excited-state dynamics. Therefore, the damping due to the shifts of the vibrational energies caused by the coupling to the rotations of the molecules is more pronounced in the excited state than in the ground-state transients.

Besides the bands at 80 and 160 cm^{-1}, the FFT spectrum of the excited-state transient (Figure 3B) shows a band at about 295 cm^{-1}. This wavenumber is about the sum of the 80 cm^{-1} vibrational spacing in the excited B state and the 208 cm^{-1} belonging to the ground-state vibrational coherence. A possible explanation is the coherence between the electronic ground and excited states due to strong laser interaction.[62] To clarify this point, quantum mechanical calculations are in progress and will be published in due time.[48]

In an effort to extend the time-resolved FWM technique to other molecules we have measured CARS transients of bromine. Very recently Averbukh et al.[63] have measured pump−probe transients of bromine. In their experiments they prepared a wave packet in the excited B state and probed the evolving dynamics by ion detection. Their intention was not to monitor the evolution of the wave packet but rather to introduce and demonstrate a general wave packet method for laser isotope separation.

In Figure 7 we show two CARS transients of bromine with different wavelength combinations, part A, $\lambda_{pu} = \lambda_{pu_r} = 548$ nm, $\lambda_S = 557$ nm, and $\lambda_{aS} = 538$ nm; and part B, $\lambda_{pu} = \lambda_{pu_r} = 535$ nm, $\lambda_S = 544$ nm, and $\lambda_{aS} = 525$ nm. The wavenumber difference between the pump and the Stokes pulse was tuned to the fundamental transition ($\Delta v' = 1$) of the Br_2 ground state vibration.

In contrast to iodine we observe only oscillations for delay times $\Delta t < 0$ (see inset in Figure 7) showing the wave packet dynamics in the excited bound B state of bromine. Analogous to iodine the pump pulse prepares the B state of bromine in a coherent superposition of a few vibrational states. This wave

packet is probed by the simultaneous pump and Stokes pulse, observing the coherent anti-Stokes Raman scattering. By varying the pump wavelength within the bound region of the B state, we observe different periods in the coherent evolution of wave packets in the B state. The period of oscillations increases as the pump energy is increased. The CARS transients show oscillations with an average period of 360 and 460 fs for the transients A and B, respectively. The oscillation periods calculated using spectroscopic data of the B state[64] are in good ageement with the observed periods.

The ratio of the intensities of the oscillations to the peak at zero time delay is considerably smaller for bromine (see Figure 7A) than for iodine (see Figure 3A). This is due to the different absorption coefficients for these two molecules reflecting the different Franck—Condon factors. The absorption coefficients for the B ← X state transitions are several orders of magnitude larger for iodine[58] than those for bromine.[65] While for iodine the resonant signal dominates the whole CARS transient, for bromine also nonresonant contributions have comparable intensities. The intense peak around zero time delay in the bromine CARS transients is due to nonresonant processes which have a very short lifetime and therefore reflect the cross correlation of the involved laser pulses.[25]

As mentioned above, transient signals for bromine could only be observed when the excited state was probed ($\Delta t < 0$). However, no oscillations could be detected for delay times $\Delta t > 0$, because of two reasons. First, the relatively large spacing of the vibrational levels in the electronic ground-state results in a poor overlap of the laser pulse shape with more than one vibrational levels. Second, the small Franck—Condon factors decrease the transition probability for the "pump—dump" preparation of the ground-state wave packet drastically.

4. Conclusions

In this study, we have employed femtosecond time-resolved CARS (coherent anti-Stokes Raman scattering) spectroscopy in order to gain information about the molecular dynamics evolving on the electronic excited as well as ground-state potential energy surface (PES). After giving a short introduction into the applied techniques, results where presented for both iodine and bromine molecules in the gas phase.

For the three laser pulses interacting with the molecular system we have chosen a three-dimensional forward geometry (folded BOXCARS arrangement). Three parameters were varied in the experiments. The wavenumber position of the pump lasers ($\tilde{\nu}_{pu}$ and $\tilde{\nu}_{pu_\tau}$) determine where the interaction with the excited-state PES takes place. The wavenumber difference between pump and Stokes lasers ($\tilde{\nu}_{pu} - \tilde{\nu}_S$) give the position accessed in the ground-state PES. The third parameter is the relative timing of the pump laser pulse pu_τ and the two other laser pulses (pu and S) which are coincident in time. If pu_τ interacts with the molecules first, it prepares a wave packet in the excited state. The dynamics of this wave packet is then probed as a function of delay time by the pu and S lasers resulting in the anti-Stokes signal at λ_{aS}. However, if pu_τ arrives at a time after the other both laser pulses have interacted with the system, the ground-state wave packet prepared by pu and S is probed.

While for iodine the dynamics on both the excited-state PES and the ground-state PES could be observed in the transient signal, the latter did not appear in the CARS transients taken from bromine. This is due to the fact that in comparison to iodine bromine has a much smaller Franck—Condon overlap for the transition between the ground X state and the excited B

state as well as a larger spacing of the vibrational levels in the ground state.

Furthermore, we have discussed the wave packet dynamics in relation to coherences. Here contributions could be found, similar to the corresponding pump—probe experiments,[56] which could be assigned to purely vibrational and rotational coherences as well as the coupling of vibrations and rotations. To separate the different vibrational and rotational contributions fast Fourier transform (FFT) calculations were performed. The rotational contribution could be subtracted from the transient yielding the modulation due to the purely vibrational coherence which was modulated by rephasing and dephasing patterns caused by the anharmonicity of the PES. Additionally, the damping of the vibrational signal due to the rotation—vibration interaction could be observed. In the FFT of the excited-state transient, besides the different vibrational transition wavenumbers within the excited state, also a contribution occurs which could be assigned tentatively to a coupling of ground and excited state vibrations. By applying a simple model, we calculated the purely rotational contribution at short time delays and fairly good agreement with the experimental results could be obtained for the excited-state transients. The model, however, was not sufficient to describe the rotational structure of the ground-state transients.

To get further information about the coherences, experiments using different polarizations for the laser pulses are planned. Additionally, the time—resolved four—wave mixing technique shall be applied to more complex molecular systems. An interpretation of the experimental results given in this paper by means of a non pertubative evaluation scheme for the nonlinear polarization will be given in a forthcoming paper.[48]

References and Notes

(1) Mourou, G., Barbara, P. F., Zewail, A. H., Knox, W. H., Eds. *Ultrafast Phenomena IX*; Springer: New York, 199.

(2) Zewail, A. H. *Femtochemistry: Ultrafast Dynamics of the Chemical Bond;* World Scientific: Singapore, 1994; Vols. I and II.

(3) Manz, J., Wöste, L., Eds.; *Femtosecond Chemistry*; VCH: Weinheim, 1995.

(4) Chergui, M., Ed.; *Femtochemistry*; World Scientific: Singapore, 1996.

(5) Rosker, M. J.; Dantus, M.; Zewail, A. H. *J. Chem. Phys.* **1988**, *89*, 6113.

(6) Zewail, A. H. *Faraday Discuss. Chem. Soc.* **1991**, *91*, 207.

(7) Berg, L.-E.; Beutter, M.; Hansson, T. *Chem. Phys. Lett.* **1996**, *253*, 327.

(8) Doany, F. E.; Hochstrasser, R. M.; Greene, B. I.; Millard, R. R. *Chem. Phys. Lett.* **1985**, *118*, 1.

(9) Laermer, F.; Elsaesser, T.; Kaiser, W. *Chem. Phys. Lett.* **1989**, *156*, 381.

(10) Kühne, T.; Vöhringer, P. *J. Chem. Phys.* **1996**, *105*, 10788.

(11) Banin, U.; Bartana, U.; Ruhman, U.; Kosloff, R. *J. Chem. Phys.* **1994**, *101*, 8461.

(12) Dai, H., Field, R. U., Eds. *Molecular Dynamics and Spectroscopy by Stimulated Emission Pumping*; World Scientific: Singapore, 1995.

(13) Baumert, T.; Pederson, S.; Zewail, A. H. *J. Phys. Chem.* **1993**, *97*, 12447.

(14) Rutz, S.; Kobe, K.; Kühling, H.; Schreiber, E.; Wöste, L. Z. *Phys. D* **1993**, *26*, 276.

(15) Knee, J. L. In *Femtosecond Chemistry*; Manz, J., Wöste, L., Eds.; VCH: Weinheim, 1995; p 167.

(16) Müller-Dethlefs, K.; Schlag, E. W. *Annu. Rev. Phys. Chem.* **1991**, *42*, 109.

Molecular Dynamics of Molecules in the Gas Phase

J. Phys. Chem. A, Vol. 102, No. 23, 1998 **4065**

(17) Mokhtari, A.; Chessnoy, J.; Laubereau, A. *Chem. Phys. Lett.* **1989**, *155*, 593.

(18) Leonhardt, R.; Holzapfel, W.; Zinth, W.; Kaiser, W. *Chem. Phys. Lett.* **1987**, *133*, 373.

(19) Bron, W. E.; Juhasz, T.; Mehta, S. *Phys. Rev. Lett.* **1989**, *62*, 1655.

(20) Fickenscher, M.; Laubereau, A. *J. Raman Spectrosc.* **1990**, *21*, 857.

(21) Okamoto, H.; Yoshihara, K. *J. Opt. Soc. Am. B* **1990**, *7*, 1702.

(22) Joo, T.; Dugan, M. A.; Albrecht, A. C. *Chem. Phys. Lett.* **1991**, *177*, 4.

(23) Fickenscher, M.; Purucker, H.-G.; Laubereau, A. *Chem. Phys. Lett.* **1992**, *191*, 182.

(24) Kaiser, W., Ed. *Ultrashort Laser Pulses*, 2nd ed.; Springer: Berlin, 1993.

(25) Hayden, C. C.; Chandler, D. W. *J. Chem. Phys.* **1995**, *103*, 10465.

(26) Heller, E. J. *Acc. Chem. Res.* **1981**, *14*, 368.

(27) Heller, E. J.; Sundberg, R. L. *J. Phys. Chem.* **1982**, *86*, 1882.

(28) Mukamel, S.; Loring, R. F. *J. Opt. Soc. Am. B* **1986**, *3*, 595.

(29) Kamalov, V. F.; Svirko, Y. P. *Chem. Phys. Lett.* **1992**, *194*, 1.

(30) Laubereau, A.; Kaiser, W. *Rev. Mod. Phys.* **1978**, *50*, 607.

(31) Abram, I. I.; Hochstrasser, R. M.; Kohl, J. E.; Semack, M. G.; White, D. *J. Chem. Phys.* **1979**, *71*, 153.

(32) Hesp, B. H.; Wiersma, D. A. *Chem. Phys. Lett.* **1980**, *75*, 423.

(33) Dlott, D. D.; Schlosser, C. L.; Chronister, E. L. *Chem. Phys. Lett.* **1982**, *90*, 386.

(34) Ho, F.; Tsay, W. S.; Trout, J.; Hochstrasser, R. M. *Chem. Phys. Lett.* **1981**, *83*, 5.

(35) Zinth, W.; Leonhardt, R.; Holzapfel, W.; Kaiser, W. *IEEE J. Quantum Electron.* **1988**, *QE-24*, 455.

(36) Zinth, W.; Kaiser, W. In *Ultrafast Laser Pulses and Applications*; Kaiser, W., Ed.; Springer: Berlin, 1988; p 235.

(37) Okamoto, H.; Yoshihara, K. *Chem. Phys. Lett.* **1991**, *177*, 568.

(38) Inaba, R.; Okamoto, H.; Yoshihara, K.; Tasumi, M. *Chem. Phys. Lett.* **1991**, *185*, 56.

(39) Purucker, H.--G.; Tunkin, V.; Laubereau, A. *J. Raman Spectrosc.* **1993**, *24*, 453.

(40) Joo, T.; Albrecht, A. C. *Chem. Phys.* **1993**, *176*, 233.

(41) Motzkus, M.; Pedersen, S.; Zewail, A. H. *J. Phys. Chem.* **1996**, *100*, 5620.

(42) Shirley, J. A.; Hall, R. J.; Eckbreth, A. C. *Opt. Lett.* **1980**, *5*, 380.

(43) Prior, Y. *Appl. Opt.* **1980**, 19, 1741.

(44) Maeda, S.; Kamisuki, T.; Adachi, Y. In *Advances in Non-Linear Spectroscopy*; Clark, R. J. H., Hester, R. E., Ed.; Wiley: Chichester, 1988; p 253.

(45) Buntine, M. A.; Chandler, D. W.; Hayden, C. C. *J. Chem. Phys.* **1992**, *97*, 707.

(46) Schmitt, M.; Knopp, G.; Materny, A.; Kiefer, W. *Chem. Phys. Lett.* **1997**, *270*, 9.

(47) Seidner, L.; Stock, G.; Domcke, W. *J. Chem. Phys.* **1995**, *103*, 39.

(48) Meyer, S.; Schmitt, M.; Materny, A.; Kiefer, W.; Engel, V. *Chem. Phys. Lett.* **1998**, in press.

(49) Ferwerda, H. A.; Terpstra, J.; Wiersma, D. A. *J. Chem. Phys.* **1989**, *91*, 3296.

(50) Myers, A. B.; Hochstrasser, R. M. *J. Chem. Phys.* **1986**, *85*, 6301.

(51) Felker, P. M.; Zewail, A. H. *J. Chem. Phys.* **1987**, *86*, 2460.

(52) Felker, P. M.; Zewail, A. H. *Adv. Chem. Phys.* **1988**, *70*, 265.

(53) Engel, V.; Metiu, H. *J. Opt. Soc. Am. B* **1990**, *7*, 1709.

(54) Hartland, G. V.; Connell, L. L.; Felker, P. M. *J. Chem. Phys.* **1991**, *94*, 7649.

(55) Hartland, G. V.; Joireman, P. W.; Connell, L. L.; Felker, P. M. *J. Chem. Phys.* **1992**, *96*, 179.

(56) Gruebele, M.; Zewail, A. H. *J. Chem. Phys.* **1992**, *98*, 425.

(57) Dantus, M.; Bowman, R. M.; Zewail, A. H. *Nature*, **1990**, *343*, 737.

(58) Tellinghuisen, J. *J. Chem. Phys.* **1973**, *58*, 2821.

(59) Barrow, R. F.; Yee, K. K. *J. Chem. Soc., Faraday Trans. 2* **1973**, *69*, 684.

(60) Coxen, J. A. *J. Quant. Spectrosc. Radiat. Transfer* **1971**, *11*, 443.

(61) Steinfeld, J. I.; Campbell, J. D.; Weiss, N. A. *J. Mol. Spectrosc.* **1969**, *29*, 204.

(62) Engel, V.; Metiu, H. *J. Chem. Phys.* **1994**, *100*, 5448.

(63) Averbukh, I. S.; Vrakking, M. J. J.; Villeneuve, D. M.; Stolow, A. *Phys. Rev. Lett.* **1996**, *77*, 3518.

(64) Barrow, R. F.; Clark, T. C.; Coxen, J. A.; Yee, K. K. *J. Mol. Spectrosc.* **1974**, *51*, 428.

(65) Passchier, A.; Christian, J. D.; Gregory, N. W. *J. Phys. Chem.* **1967**, *71*, 937.